Nanocomposite pervaporation membrane for desalination

by Indah Prihatiningtyas

Submission date: 17-Mar-2022 12:27PM (UTC+0700)
Submission ID: 1786160416
File name: review_article_ChERD.pdf (1.92M)
Word count: 13805
Character count: 71479

Chemical Engineering Research and Design 164 (2020) 147–161

Contents lists available at ScienceDirect

Chemical Engineering Research and Design

journal homepage: www.elsevier.com/locate/cherd

Nanocomposite pervaporation membrane for desalination

Indah Prihatiningtyas[a,b,*], *Bart Van der Bruggen*[a,c,*]

[a] *Department of Chemical Engineering, KU Leuven, Celestijnenlaan 200F, B-3001, Leuven, Belgium*
[b] *Department of Chemical Engineering, Mulawarman University, Jalan Sambaliung No. 9, Sempaja Selatan, Samarinda, Kalimantan Timur, Indonesia*
[c] *Faculty of Engineering and the Built Environment, Tshwane University of Technology, Private Bag X680, Pretoria 0001, South Africa*

ARTICLE INFO

Article history:
Received 10 July 2020
Received in revised form 30 September 2020
Accepted 5 October 2020
Available online 12 October 2020

Keywords:
Pervaporation
Desalination
Nanocomposite membrane

ABSTRACT

Desalination via pervaporation has been considered as an attractive membrane process for obtaining clean water from non-potable saline sources, which has advantages, i.e., it is superior in salt rejection and has the capability of coping with high-salinity feed solutions. In the pervaporation process, the membrane material plays the key factor because it is governing the overall efficiency. This overview of nanocomposite pervaporation membranes for desalination mostly emphasizes on membrane materials, the effect of operating parameters on pervaporation performance, and the current research towards the development of nanocomposite membrane. Nearly all types of membranes ever stated in pervaporation desalination are mentioned, based on polymers, inorganic materials and hybrid organic-inorganic materials (nanocomposite) with their performance in terms of water flux and salt rejection.

1. Introduction

Water is one of the fundamental conditions required for organisms to survive. However, during the last few decades, the rapid world population, rising living standard, consumption pattern changes, climate change, extension of irrigated agriculture and industrialization are driving for an escalating global demand for clean water, which leads to water scarcity (Vörösmarty et al., 2000; Ercin and Hoekstra, 2014; Elimelech and Phillip, 2011). Encouraging efforts to overcome the lack of clean water have been made by the development of water treatment processes in the 20th century; however, water scarcity is much more pressing today than before. The World Water Council (WWC) has estimated that 3.9 billion people in the world will live in water-scarce areas by 2030 (WWC, Urban Urgency, Water Caucus Summary, 2007). Along similar lines, the World Health Organization (WHO) predicted that 2.1 billion people lack of safe drinking water supply (WHO, Water, Sanitation and Hygiene strategy 2018–2025, 2018) (Li et al., 2019). Therefore, the provision of clean water has become a major issue for public and government. Water resources on earth comprise conventional water resources (CWRs) and unconventional water resources (UCWRs). CWRs are groundwater, rivers and lakes, while UCWRs involve seawater, brackish water and wastewater, which evidently requires much more purification before it can be used.

The total water supply (both salt and freshwater) on the earth is 1.4 billion km^3, of which 97.5% is saltwater, which cannot be used directly for human consumption (Hameeteman, 2013). Hence desalination, which converts salty water to fresh water from the almost limitless source of seawater, has become an attractive solution to deliver clean water to the community. There are two major types of technologies for desalination: thermal desalination and membrane technology. In recent years membrane technology has become the most attractive option for desalination due to its advantages, such as its high efficiency and energy saving (Semiat, 2008; Drioli et al., 2011), high operational stability, low chemical costs, easy to integrate and control within industrial processes (Drioli et al., 2011). Since reverse osmosis (RO) membranes were developed in the1960s, membrane technology

* *Corresponding authors at*: Department of Chemical Engineering, KU Leuven, Celestijnenlaan 200F, B-3001, Leuven, Belgium.
E-mail addresses: indahprihatiningtyas.yamsidi@kuleuven.be (I. Prihatiningtyas), bart.vanderbruggen@kuleuven.be (B. Van der Bruggen).
https://doi.org/10.1016/j.cherd.2020.10.005
0263-8762/

has taken over the desalination market with installed 73% membrane-based desalination while 27% is thermal desalination (Ahmed et al., 2019). RO is a mature technology for supplying fresh water from seawater (salinity of 3.5 wt%) and brackish water (salinity of 0.05–3 wt%) primarily due to its low cost and high salt rejection of over 99.5% (Li, 2016). RO has so far maintained its leadership among alternative membrane processes such as membrane distillation (Hsu et al., 2002), electrodialysis (Sadrzadeh and Mohammadi, 2008), capacitive deionization (Oren, 2008) and forward osmosis (McGinnis and Elimelech, 2007) that have been proposed (Lee et al., 2011). However, RO has certain drawbacks: the driving force needs to be increased to handle highly concentrated salt water, which leads to higher cost, and RO membrane elements are sensitive to fouling. To address these issues, innovative membrane technologies are proposed to improve the established membrane processes for desalination.

Pervaporation (PV) is a thermal driven membrane processes (Xue et al., 2020), in which the chemical potential difference acts as driving force (Cannilla et al., 2017; Slater et al., 2006). PV has attracted many researchers to be developed as a potential desalination method due to some advantages such as a potential low energy, high salt selectivity, limited effects of fouling, and the capability to handle feed waters with high salinity (Prihatiningtyas et al., 2020a; Wang et al., 2016). Limited information on the application of pervaporation for desalination and wastewater treatment might be due the lack of a high water flux in PV compared to RO. Most efforts of researchers are devoted to searching the right PV desalination membrane material to achieve the preferred separation in an efficient way. An ideal PV membrane should have a high water flux and selectivity, good mechanical and thermal resistance, and have a good fouling resistance, leading to a long lifetime. A study reported that chlorination to prevent biofouling of RO membranes is an issue due to the active chlorine attacks polymer network of RO (Al-Abri et al., 2019), for example the applications of polyamide thin film composite (PA-TFC RO) membranes for desalination (Xu et al., 2013). Typical PV membranes are hydrophilic membrane which the dense selective layer is a good fouling resistance, however Li et al. found that PV desalination membranes showed gradually deteriorated desalination properties due to a fouling (Li et al., 2017). Hence, Zhao et al. studied to modify polyvinyl alcohol (PVA) polymer with a fluorine based crosslinker (FS-3100) to increase the chlorine resistance. They reported that the fabricated composite membranes showed much better chemical resistances to acid, alkali, and also chlorine solutions (Zhao et al., 2020).

PV membranes are dense; they are made of polymers such as polyether amide, sulfonated polyethylene, poly(vinyl alcohol), and cellulose-based material (Wang et al., 2016); however, they have some limitations such as low permeability, high energy consumption, low resistance to fouling, and short life span (Alaei Shahmirzadi and Kargari, 2018). Hence the development of new membrane materials to obtain a PV membrane with desired properties, energy efficient, and cost effective is needed for desalination. Researchers have been introducing nanoparticles into a polymer matrix to overcome the challenges of the present polymeric PV membranes. Nanoparticles such as silica, zeolite, alumina, clay, TiO_2, MoS_2, graphene oxide, carbon dots, carbon nanotubes (CNTs), and multi-walled carbon nanotubes (MWNTs) have been employed to prepare desalination membranes (Prihatiningtyas et al., 2020a). Although nanoparticles provide extraordinary benefits, there are some challenges in membrane fabrication for industrial development. Therefore, this article reviews the current research progress in nanocomposite pervaporation membranes for desalination from the viewpoints of membrane materials and membrane fabrication procedures.

2. Pervaporation desalination

Pervaporation is a membrane process developed to separate liquid mixtures based on selective sorption and diffusion of one of the species through the dense membrane. The term pervaporation was defined by Kober as a contraction of 'permeation' and 'evaporation', after observing the selective permeation of water through a collodion and parchment membrane at the 1910s (Kober, 1917). In pervaporation, a liquid mixture in the feed is contacted with one side of a membrane, then the product in the permeate side is collected in a vapor form (Luis, 2018). Fig. 1 shows the pervaporation process.

Gesellschaft für Trenntechnik (GFT) ventured to launch the first commercial PV membrane by fabricated composite membrane where a thin layer of crosslinked polyvinyl alcohol (PVA) was coated on a porous poly(acrylonitrile) (PAN) support cast on anon-woven fabric (Tusel and Brüschke, 1985). Further the first pervaporation plant for dehydration of ethanol in industrial scale was established in Brazil in 1983, then followed by others (Brüschke, 2006). Pervaporation was successfully applied for separating simple alcohols from their mixture with organic solvents. The first industrial plant was in 1997 which separating methanol from methylester (Maus and Brüschke, 2002). Pervaporation has been recently interesting to be applied for other separations such as removal of low volatile organic components (VOCs) from aqueous stream (Kujawa et al., 2015) and desalination (Wang et al., 2016).

Since the 1990s, studies on pervaporation for desalination were focused on transport mechanisms, membrane materials and membrane performance under various operating conditions with the aim of exploring PV as an innovative and efficient desalination technique (Wang et al., 2016). In pervaporation desalination, the feed (aqueous salt solution) is heated up to the operating temperature, and brought to contact with a perm-selective membrane so that the permeated product (water in the form of vapor) is continuously removed from the permeate (Xie et al., 2018). There are three PV configurations that are most used to remove the vapor in pervaporation, i.e., vacuum PV, air sweep PV and air gap PV. Vacuum PV and air sweep PV are the most generally applied. In vacuum PV, a vacuum and a liquid nitrogen cold trap are used, while in air sweep PV an inert sweeping air is used to remove water vapor from the membrane surface in the permeate side (Wang et al., 2016). Currently, also another PV configuration has been used for desalination, i.e., direct contact PV desalination (DCPV) (Meng et al., 2019, 2020). Meng et al. (2019) reported that DCPV shows potential for pervaporation desalination because it is easy to scale-up. Fig. 2 shows the typical PV configurations vacuum PV, air sweep PV, air gap PV, and direct contact PV.

2.1. *Fundamentals of the pervaporation desalination process*

A single explanation for the passage of components through a PV membrane is difficult to be formulated because of the complex interaction between feed, penetrants, and membrane. Hence there is no universal model that can describe each part of mass transport in PV membranes then result in a specific transport model (Shao and Huang, 2007). Mass transfer models in PV are generally depending on the material and structure of the membrane. Diffusion through a dense membrane (normally a non-porous uncharged polymeric membrane) is defined by the solution-diffusion (Korngold et al., 1996; Huth et al., 2014; Liang et al., 2014; Xie et al., 2014); the pore-flow model is used for a porous membrane (usually inorganic membranes) (Wang et al., 2016). Thermodynamic and kinetic aspects should be considered for the permeation of a component through a PV membrane. Thermodynamics determine the solubility, while kinetics determine the diffusion of the penetrant through the membrane (Ong et al., 2016). Fig. 3 illus-

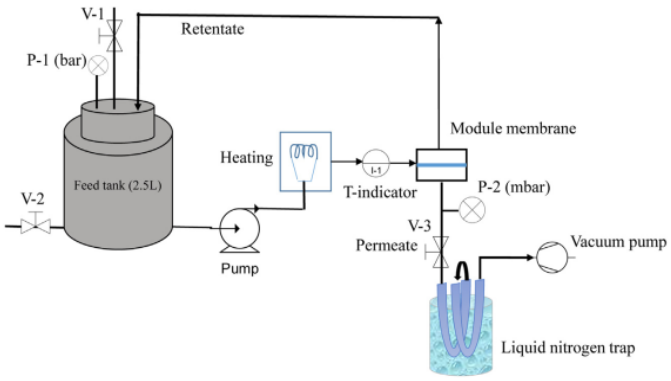

Fig. 1 – Pervaporation process.

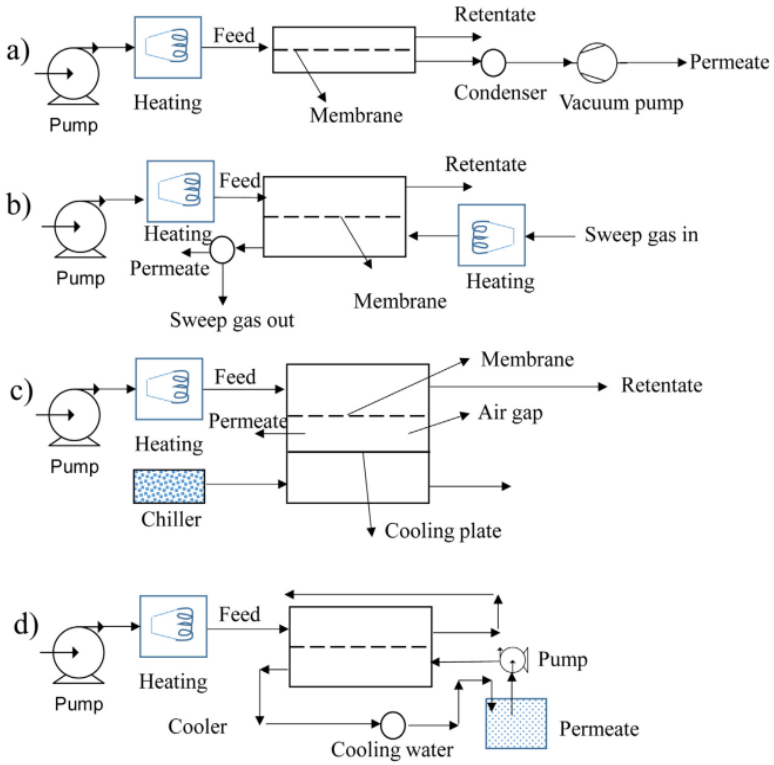

Fig. 2 – Different Pervaporation (PV) configurations: (a) Vacuum PV, (b) Air sweep PV, (c) Air gap PV, and (d) Direct contact PV.

trates the model of solution-diffusion, which consists of three steps: (i) Sorption of the permeating species from the feed liquid into the selective membrane surface; (ii) Diffusion of the permeating species across the membrane; (iii) Desorption of the permeating species as vapor on the permeate side of the membrane (Feng and Huang, 1997).

Hence, the elucidation for PV desalination is proposed that water molecules are specially dissolved/adsorbed, then diffuse through the membrane while salts are rejected by a dense membrane. Productivity and capability in separating the components from the feed mixture are generally used to assess the performance of a PV desalination which characterized in terms of water flux and salt rejection. The water flux (J) and salt rejection (R) can be defined as:

$$J = \left(\frac{M}{A\,x\,t}\right) \quad (1)$$

$$R = \left(\frac{C_{f-C_p}}{C_f}\right) \quad (2)$$

where M is the amount of permeate collected in a condenser (kg), A is the effective membrane area (m^2), t is the PV time

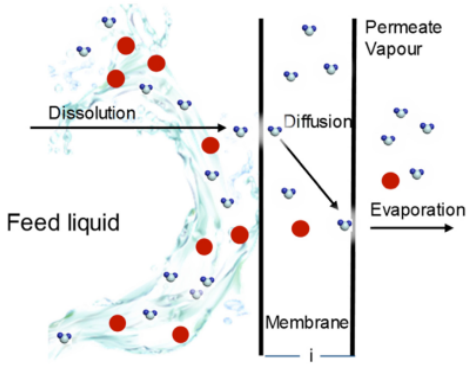

Fig. 3 – Solution diffusion in pervaporation.

(h), and C_f and C_p are the salt concentrations in the feed and the permeate, respectively.

In the solution diffusion mechanism, it has been reported that facilitated transport enhances the water flux by immobilized liquid films, swollen polymers (Saeed et al., 2017), and reactive functional groups decorated on the solid polymer film (Xue et al., 2019). Xue et al. studied the facilitated water transport mechanism in crosslinked polyvinyl alcohol (PVA). Molecular dynamic (MD) simulations results showed that a higher 4-sulfophthalic acid (SPTA) increased the movement of water molecules and also their interactions. Hence, in pervaporation, sulfonic acid groups are used as fixed facilitate transport agents (Xue et al., 2019). Fig. 4 illustrates the transport mechanisms for water molecules in the membrane by solution–diffusion mechanism and facilitated transport.

2.2. *Operation parameters*

The performance of a pervaporation membrane for desalination depends on several parameters: feed salt concentration, feed temperature, feed flow rate, permeate vapor pressure, and sweep velocity (Wang et al., 2016).

1 Feed salt concentration

Xie et al. revealed that at high temperatures (50 °C), the effect of salt concentration on water flux was significant, while at room temperature (20 °C), it was negligible (Xie et al., 2011a). This is because the partial vapor pressure at room temperature at different salt concentrations is not significantly different, but at higher temperatures, it is directly proportional to the temperature. Prihatiningtyas et al. discovered that increasing NaCl in feed solution from 0 to 90 g/L decreased the water flux by 30%, while increasing the NaCl concentration from 30 to 90 g/L reduced the water flux by 25% (Prihatiningtyas et al., 2020b). The cause for the decreased water flux is that the water concentration in the feed solution decreases along with increasing of NaCl concentration, which later diminishes the water sorption on the membrane interface (Wu et al., 2018). Furthermore, a higher NaCl concentration in the feed solution might result in membrane fouling and concentration polarization on the membrane surface, which decreases the water flux (Huth et al., 2014; Liang et al., 2015).

2 Feed temperature

It has been reported that the water flux increases exponentially with feed temperature for all feed concentrations (Liang et al., 2014; Xie et al., 2011a; Prihatiningtyas et al., 2020b; Zwijnenberg et al., 2005; Malekpour et al., 2008). Liang et al. found that an increment of temperature from 30 °C to 90 °C enhanced the water flux from 14.3 kg m^{-2} h^{-1} to 65.1 kg m^{-2} h^{-1} in pervaporation desalination for 35 g/L of NaCl in the feed solution (Liang et al., 2015). Prihatiningtyas et al. discovered that the water flux doubled when the temperature was elevated from 40 °C to 70 °C in a feed solution containing 90 g/L of NaCl (Prihatiningtyas et al., 2020b). Several factors are responsible the increment of water flux with feed temperature. First, increasing feed temperature will increase feed water vapor pressure, which leads to an increase in water flux. While the vapor pressure on the permeate side stays constant, leading to an increase of the driving force, which consequently enhances the water flux (Xie et al., 2011a). Second, the diffusion coefficient of water increases with temperature, which facilitates that water can penetrate the membrane. Xie et al. reported that when the temperature increased from 20 °C to 65 °C, the diffusion coefficient of water increased up to 350% at 2 g/L of NaCl in the feed solution, while at high salinity (50 g/L of NaCl), it improved by 200% (Xie et al., 2011a). Third, the temperature increase results in a larger free volume in the membrane polymer; the water molecules diffuse through the free volume more easily (Burshe et al., 1997). This is according to the free volume theory, that the thermal motion of polymer chains in the amorphous region generates momentary free volumes; these free volumes become larger due to the frequency and amplitude of the chain motion (i.e., thermal agitation) due to the increasing temperature. Theoretically, the Arrhenius relationship can be used to understand the relation between water flux and temperature (Yeom and Lee, 1997; Peng et al., 2006; Jiraratananon et al., 2002).

$$J_i = J_o \exp\left(-\frac{E_{j,i}}{RT}\right) \quad (3)$$

where J_i is the water flux of i, J_o is the pre-exponential factor, R is the gas constant, T is the absolute temperature and $E_{j,i}$ is the apparent activation energy for permeation.

3 Feed flow rate

Theoretically, an increment of feed flow rate will result in increasing of water flux due to the concentration polarization near the feed interface reduced. Decrease in water concentration near the feed interface/membrane which approaches the water concentration in the bulk, it will create more water can be adsorbed on the membrane surface which lead the water flux is increased. Besides, decreased polarization concentration will reduce the transport resistance in the liquid boundary layer, then generates the water flux increased (Wang et al., 2016). Liu et al. studied the removal of volatile organic compounds (VOCs) from contaminated groundwater by pervaporation (Liu et al., 2003). The simulation results showed that the concentration polarization index (CPI) decreased with the increase of feed velocity, while the results of the relationship between feed concentration and permeation flux followed a linear regression equation. However, Xie et al. (2011a) discovered that that the water flux of a hybrid PVA/MA/silica membrane stayed constant at around 2.5 kg.m^{-2}.h^{-1} on varying the feed flow rate of 30–150 ml/min at temperature 22 °C. This is because the increasing feed the flow rate within the

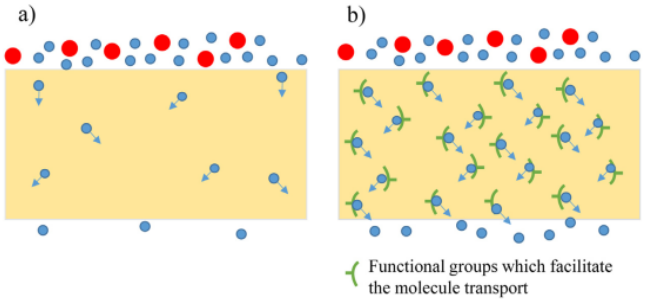

Fig. 4 – Transport mechanisms for water molecules in the membrane: (a) Solution–diffusion mechanism and (b) facilitated transport mechanism.

laminar flow regime (i.e. Reynolds number b 2000) will not take a significant function in the increment of water flux due to the little or negligible effect of the turbulence and fluid dynamics of the feed. In addition, Borisov et al. in their studies reported that increasing feed temperature will decrease the boundary layer (Borisov et al., 2018). The boundary layer thickness also reduced with an enhancement in the feed flow rate (Borisov et al., 2018; Wijmans et al., 1996). Borisov et al. found that the boundary layer thickness dropped when the feed flow rate increased from 4 to 30 $dm^3\ h^{-1}$ which indicated that the hydrodynamic regime changed under these conditions. In contrast, at flow rates in the range of 30–70 $dm^3\ h^{-1}$, the boundary layer was mainly affected by the intrinsic enrichment factor and the permeate flux. Hence, an increasing velocity resulted in a slight change of the boundary layer thickness. Furthermore, it was reported that the boundary layer thickness turned to zero at an operating temperature of 50 °C and a feed velocity of 1.34 cm s^{-1}.

4 Permeate pressure

Mass transport in pervaporation is driven by a vapor pressure gradient (ΔVP) between the feed and permeate side. A high ΔVP is obtained by keeping a low absolute pressure in the permeate stream, hence the permeate pressure become important operating parameter because a high vacuum is related to a high energy charge. With increasing the vacuum (i.e., decreasing the permeate pressure), the transmembrane vapor pressure difference is decreased, which causes an enhanced driving force and an increases water flux (Xie et al., 2011a). Xie et al. reported that when the vapor pressure in the permeate increased from 2 to 15 Torr, the water flux decreased by 90% from 3 kg $m^{-2}\ h^{-1}$ to 0.3 kg $m^{-2}\ h^{-1}$ (Xie et al., 2011a). Huth et al. reported that the water flux of a commercial cellulose triacetate membrane increased by 400% when the vapor pressure gradient increased from 2.3 kPa to 12.275 kPa, while the flux of a commercial polyester membrane with thickness of 20 μm enhanced by approximately 150% (Huth et al., 2014).

5 Sweep velocity

Pervaporation desalination utilizes hydrophilic membranes. The typical effect of air velocity in air-sweep PV is that at lower sweep velocity, the water flux will increase along with an elevation of air velocity. However, the water flux is independent of the air velocity at high certain value, because the limiting factor is the water diffusion in the membrane (Korngold et al., 1996; Korngold and Korin, 1993; Korin et al., 1996; Quiñones-Bolaños et al., 2005). Korin et al. found that the water flux enhanced when the air velocity increased up to 2.0 m s^{-1}, however, the resistance to transport of the water vapor was insignificant after approaching 2.0 m s^{-1}, hence the flux remained constant (Korin et al., 1996). Korngold et al. confirmed that the water flux depended on air velocity at low air velocities, i.e., 1.5 m s^{-1}, while above 2.0 m s^{-1}, it depended on the transport of liquid water through the membrane (Korngold et al., 1996). Furthermore, Balanos et al. discovered that the water flux rose with the increment of sweeping air-Re until 1200 for a hollow fiber membrane, and up to 2000 for a corrugated sheet membrane (Quiñones-Bolaños et al., 2005). Generally, an enhancement of the air–sweep velocity reduces the water concentration at the permeate side of the membrane, so that the gradient driving force through the membrane increases, resulting in a higher water flux.

2.3. *Membrane thickness*

In addition to the operating conditions mentioned above, membrane thickness also influences the membrane performance. Theoretically, transport of water molecules through the membrane follows the solution-diffusion model, in which according to Fick's equation, the water flux is inversely proportional to membrane thickness (Wang et al., 2016).

$$J_i = \frac{D_i\left(C_{if(m)} - C_{ip(m)}\right)}{l} \tag{4}$$

where D_i is the diffusion coefficient of component i in the membrane ($m^2\ s^{-1}$), and l is the membrane thickness (m). $C_{if}(m)$ means the concentration of component i in the feed side (kg m^{-3}) and $C_{ip}(m)$ in the permeate side (kg m^{-3}).

The water flux decreases with increasing membrane thickness because the permeation resistance enhances when the membrane thickness increased. Huth et al. studied the feasibility of pervaporation for desalinating high-salinity brines, and concluded that the flux increased by a factor 2.5 (from 3.73×10^{-7} to 1.37×10^{-6} $m^3\ m^{-2}\ day^{-1}\ Pa^{-1}$) when the membrane thickness decreased from 250 μm to 200 μm (Huth et al., 2014). Prihatiningtyas et al. reported that the water flux enhanced by a factor 2 (from 5.76 kg $m^{-2}\ h^{-1}$ to 11.68 kg $m^{-2}\ h^{-1}$) when the casting blade height reduced from 200 to 100 μm (Prihatiningtyas et al., 2019).

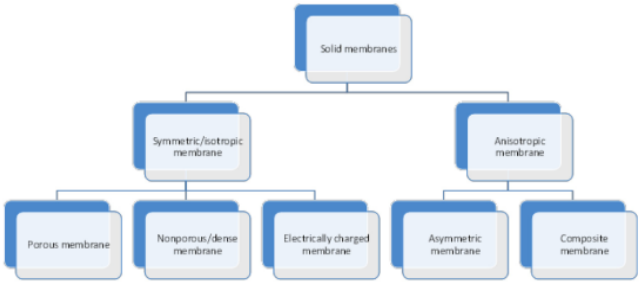

Fig. 5 – Solid membrane classifications based on morphology.

3. Pervaporation membrane

3.1. *Fabrication method*

Membranes are a selective barrier in a separation process that is permitting a certain compound through their structures by a combination of sieving and diffusion mechanisms. Membrane can be in the form of a solid or a liquid. Solid membranes are classified as shown in Fig. 5 (Purkait et al., 2018).

Symmetric membranes can be of three types, based on the membrane structure (Purkait et al., 2018):

1 Porous membranes: These membranes are defined as having pores. In general, the separation is a function of molecular size. These membranes are mainly employed for ultrafiltration and microfiltration.
2 Nonporous or dense membranes: These membranes consist of a dense structure in which the pores are unable to be detected at the limits of electron microscopy. Mass transport is governed by diffusion or a pressure, concentration, or electrical potential gradient as driving force. Transport is governed by diffusivity and solubility in the membrane material. Pervaporation and reverse osmosis are generally using these membranes.
3 Electrically charged membranes: These membrane can be dense or microporous, but most generally are very finely microporous, with the pore walls carrying fixed positively or negatively charged ions. These membranes are referred to as ion-exchange membranes and have been used in electro dialysis.

While anisotropic membranes are explained as following (Purkait et al., 2018):

1 Asymmetric membranes: These membranes consist of two main layers. A selective skin layer on the top is very dense and a support layer is porous. These membranes are mostly used for ultrafiltration, nanofiltration, and reverse osmosis.
2 Composite membranes: These membranes are generally made by the deposition of a thin top-layer on a porous sublayer from different polymers in each layer. The properties of each layer can be optimized independently to achieve the required selectivity, permeability, chemical and thermal stability. The separation properties and permeation rates of the membrane are assigned by the top layer, while the sublayer functions as a mechanical support.

Membranes in PV act as a molecular selective layer between the feed solution and the permeate. Membranes for pervaporation are generally dense or asymmetric with a thin dense film acting as a selective layer. Dense membranes are commonly resulting a moderately low water flux. In contrast, asymmetric membranes have a thin selective layer on a relatively thick microporous substrate, in which the microporous structure increases the water flux due to the reduced transport resistance (Ong et al., 2016). The following methods are employed for fabricating pervaporation membranes (Roy and Singha, 2017):

1 Solution casting

Solution casting is a commonly used method for fabricating flat-sheet membranes for various membrane applications. Firstly, a polymer solution is prepared by dissolving a polymer and all other necessary ingredients in a solvent until homogeneous. Then the membrane film is fabricated by spreading the polymer solution onto a flat glass plate or Petri dish followed by evaporation and/or phase inversion to remove the solvent. Dense membranes are prepared by evaporation, while asymmetric membranes are made by phase inversion with immersion in a non-solvent bath. The dried membrane is peeled off from the glass support after complete evaporation of solvent. Fig. 6 illustrates the solution casting method for fabricating nanocomposite membranes.

2 Solution coating

Composite membranes are commonly fabricated by solution coating. A thin selective layer is deposited on top of microporous substrates or supports (flat-sheet, hollow fiber or tubular configuration). However, most PV desalination membranes are in the flat-sheet configuration. The membrane resistance is primarily controlled by the coated selective layer, hence the porous substrate can reduce the substructure resistance (Li et al., 2013a; Shieh et al., 1999; Yave et al., 2010). Fig. 7 describes the solution coating method.

3 Spray coating

Spray coating is a possible technique in preparing thin film composite (TFC) and thin film nanofibrous composite (TFNC) membranes (Wang et al., 2017). Spray coating has been applied to prepare membranes, for example, Acharya et al. used spray coating to prepare nanoporous carbon membranes from poly(furfuryl) alcohol on stainless steel, which were then applied for separating oxygen and nitrogen (Acharya and Foley, 1999). Xue et al. employed a spray coating method to prepare a thin film of polyvinyl alcohol (PVA) as membrane

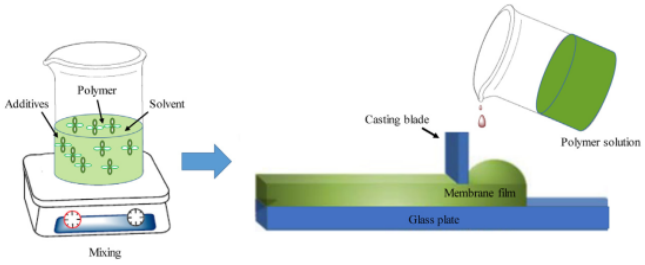

Fig. 6 – Solution casting method.

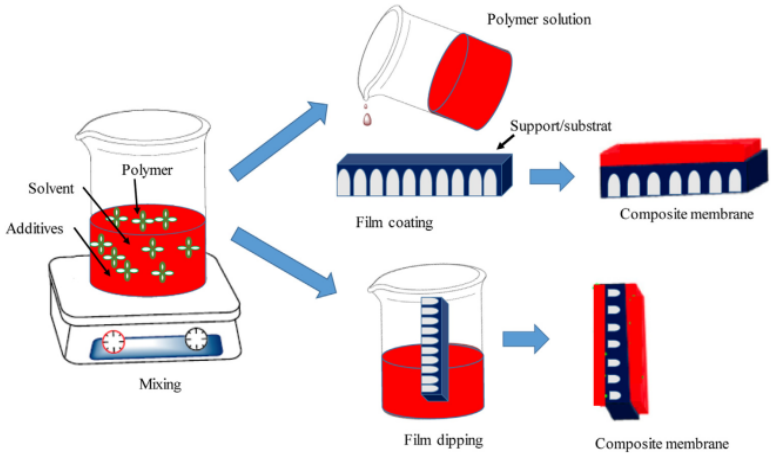

Fig. 7 – Solution coating method.

for pervaporation desalination. The desalination performance showed positive with spray coating of 0.73 μm thick (Xue et al., 2020). Meng et al. used spray coating to overcome the incompatibility between hydrophobic polymers and hydrophilic polymers for desalination application. They found that the spray coated PVA/polytetrafluoroethylene (PTFE) membrane in direct contact membrane distillation (DCMD) mode obtaining water flux of 64.2 + 2.9 kg m^{-2} h^{-1} with salt rejection above 99.9% (Meng et al., 2019).

4 Hollow fiber spinning

In this method, the membrane is produced through phase inversion. The polymer solution is extruded simultaneously with the bore fluid in the lumen side of the nascent fiber. After the nascent fiber appears from the spinneret, coagulation immediately occurs at its internal surface. The entire phase inversion process is finished when the fiber is totally precipitated in the external coagulation bath. The thickness and morphology of the selective membrane layer can be controlled by changing compositions of the dope solution, bore fluid, external coagulant, and the speed.

5 Interfacial polymerization

Interfacial polymerization is a reaction between the polycondensation of diamine and diacid chloride monomers to form polyamide and hydrogen chloride, which initially proposed by Wittbecker and Morgan (1959). Using interfacial polymerization to fabricate the PV membranes, very thin selective layer will be formed on top of the substrate, which significantly enhances the membrane flux. Chemical resistance, thermal stability and long term durability of the thin selective layer can be improved by choosing appropriate monomers for the interfacial polymerization (La et al., 2010). Cui et al. have studied the preparation of an acid-resistant polysulfonamide/polyethersulfone composite membranes by interfacial polymerization for desalination pervaporation (Cui et al., 2020). The interfacial polymerization on polysulfonamide dense membrane employed an aqueous solution containing m-phenylenediamine (MPD) and triethylenetetramine (TETA) with 1,3-benzenedisulfonyl chloride (BDSC) as an organic solution. The results showed that the prepared membrane survived at acid condition as the water flux was stable during pervaporation for over a 600 min at 10 wt% H_2SO_4 solution at feed temperature of 75°.

6 Physicochemical modifications

Post-modification processes are generally employed to increase the performance and stability of PV membranes. Pervaporation membranes for desalination should be hydrophilic. Incorporating or grafting appropriate functional groups into the polymer chains can be utilized to modify the membrane hydrophilicity, in order to improve the affinity between water molecules and the membranes. In addition, post-annealing can be applied to reduce potential defects on the selective layer of the membranes (Ong et al., 2016).

3.2. *Organic and inorganic pervaporation membranes for desalination*

The most important factor in pervaporation is the membrane itself. Therefore various materials have been developed for pervaporation desalination membranes. The primary materials employed for fabricating PV desalination membranes are organic polymers such as polyethylene (PE) and cellulose based materials. Microporous inorganic membranes such as zeolites and amorphous silica-based membranes started to gain interest to be developed for PV desalination membranes in the late 2000s. Generally, polymeric membranes are easy to process, have a good mechanical stability, and are cost effective; however their drawback is in the low chemical and thermal stability, and particularly the characteristic trade-off relation between permeability and selectivity (highly permeable membranes have a low selectivity and vice versa) (Roy and Singha, 2017). In contrast, inorganic membranes commonly have a superior separation performance, but these membranes are expensive and difficult to fabricate as defect-free continuous layers on large scale. The polymeric and inorganic, and hybrid organic-inorganic PV membranes for desalination reported so far are summarized in Table 1.

3.3. *Nanocomposite membrane for pervaporation desalination*

Hybrid organic-inorganic membrane materials have been developed by combining an organic phase and an inorganic phase through chemical bonding to overcome the drawbacks of polymers and inorganic PV membranes. Recently, polymer nanocomposite membranes obtained by dispersing nanomaterials in a polymer matrix have been considered as having the highest potential to be developed for liquid–solid, gas–gas, and liquid–liquid separations (Zahid et al., 2018). Nanocomposite membranes are interesting for PV desalination because they may overcome the trade-off between permeability and solute rejection; they are of interest for manufacturing the next generation high-performance membranes for PV desalination. Nano-fillers/nanomaterials employed in nanocomposite membranes are organic materials, inorganic materials, hybrid materials (two or more material types) and biomaterials. The addition of fillers into polymer membranes tends to change the membrane surface properties affecting the separation performance. Generally, polymer nanocomposite membranes in either hollow fiber or flat sheet configuration are fabricated by phase inversion (Zahid et al., 2018).

Polymer nanocomposite membranes are classified into two types: thin-film nanocomposite membranes and blended nanocomposite membranes. It has been reported that the structure of the support layer of a composite membrane has a significant impact on the water flux in PV desalination. The water flux can be improved by either reducing the thickness of the selective layer or decreasing the support layer resistance (Li et al., 2018). Li et al. have investigated this by optimizing the support layer structure to decrease its resistance to water vapor transport (Li et al., 2018). The results showed that the best support layer of polysulfone (PSF) was prepared at a RH of 5% and LiCl concentration of 2 wt%, which improved the water flux by 31% compared to a previous study using polyacrylonitrile (PAN) as support layer (Liang et al., 2018).

In blended nanocomposite membranes, the casting solution is prepared by dispersing nanoparticles along with polymer and additives prior to casting on a flat surface. Commonly, nanoparticles are added into the casting solution to fabricate PV nanocomposite membranes for desalination a to modify the morphology and performance of the membrane, often in view of increasing the hydrophilicity of the membrane (Shahmirzadi and Kargari, 2018). Nanocomposite membranes produced by the blending method are nanoparticles entrapped membranes or nanoparticles blended membranes (Zahid et al., 2018). Thin film nanocomposite (TFN) membranes are fabricated by incorporating nanoparticles within the thin film formed on the membrane surface through dip-coating or deposited on support or substrate with pressure (Vatanpour et al., 2012). Employing nanoparticles in TFN membranes aims at modifying the properties of the surface thin layer in order to improve the hydrophilicity and/or surface charge density without sacrificing the selectivity (Lau et al., 2015).

3.3.1. *Nanoparticles to enhance performance of pervaporation desalination membrane*

Modification of membrane materials by incorporating nanomaterials to produce nanocomposite membranes has been found a promising way to enhance the membrane performance. Incorporating nanoparticles into a polymer generally tends to change the membrane properties affecting the separation performance, e.g., high permeability and selectivity, improved hydrophilicity and mechanical strength, enhanced antifouling behavior and antibacterial properties, and better thermal stability (Ng et al., 2013). Nanoparticles for membrane desalination applications are interesting due to their unique structural and morphological features, which result in rapid water transport and high salt rejection. There are numerous studies that have employed different nanoparticles (NPs) to fabricate nanocomposite PV membranes for desalination, such as silica (SiO_2) (da Silva et al., 2020), graphene oxide (GO) (Liang et al., 2015), carbon nanotubes (CNTs) (Yang et al., 2019), MXene (Liu et al., 2018), nano clay-laponite (Selim et al., 2019), cellulose nanocrystal (CNCs) (Prihatiningtyas et al., 2019), and aluminum oxide (Al_2O_3) (Prihatiningtyas et al., 2020b).

1 Silicon dioxide (SiO_2)

Many studies have used silicon dioxide NPs for drinking water treatment since are less toxic to the environment compared to silver and copper NPs (Taha et al., 2012). For better NPs dispersion in solvents, surface modification/functionalization of NPs has been done in order to enhance the surface charge (Kim et al., 2015). Wu et al. modified the surface of SiO_2 NPs with a silane coupling agent to reduce agglomeration, and then decorated them with a polydimethylsiloxane (PDMS) chain. The modified SiO_2 facilitates migration of PDMS or polyethylene glycol (PEG) to membrane surface and enhances the stability of the additives in the membrane (Wu et al., 2012).

Moreover, incorporating functionalized SiO2 into nanocomposite membranes was reported to elevate hydrophilicity and water absorption (Han et al., 2011). Nanosilica is a nano-hydrophilic additive due to the presence of —OH groups in silanols (Rallini and Kenny, 2017). In addition, SiO_2 NPs also have a propensity to increase the thermal stability of composite membranes due to the tough interaction with the polymer matrix (Rahman and Padavettan, 2012; Sani et al., 2015). The presence of SiO_2 NPs in a polymer membrane changes the membrane morphology, generating the microstructure or nanostructure which leads to enhanced physical properties and performance (Xie et al., 2011b). However, Lalia et al. at reported that increasing the

Table 1 – Polymeric and inorganic of PV membranes for desalination.

Membrane	NaCl (g/L)	Operating condition in feed side	Condition in permeate side	Membrane thickness (μm)	Flux (kg/m².h)	Rejection (%)	Ref.
Organic polymer							
Sulfonated polyethylene	0–176	25–65 °C	Air sweep	100	3.3–0.8	-	Korin et al. (1996)
Sulfonated polyethylene	35	45–65 °C	Air sweep	50–180	3–1.5	-	Korngold et al. (1996)
Polyether ester	3.2–30	22–28.7 °C 15–20 kPa 500 ml/min	Air sweep	160	0.146–0.12	80	Quiñones-Bolaños et al. (2005)
	0.85–16.8	22–28.7 °C 20–35 kPa 500 ml/min	Air Sweep	180	0.108–0.096	80	Quiñones-Bolaños et al. (2005)
Polyether amid	30	68–70 °C	Cooler tunnel	40	0.2	99.98	Zwijnenberg et al. (2005)
Polyester	35–70	Room temperature	The membrane tube was placed in sand	750	7.1–5	99.91–99.84	Sule et al. (2013)
Polyester	100	50 °C	Air sweep	20	54	99	Huth et al. (2014)
Cotton cellulose	40	40 °C	Vacuum	30	6.7	100	Kuznetsov et al. (2007)
Cellulose diacetate on polytetrafluoethylene	40	40 °C	Vacuum	3.5	5.1	100	Kuznetsov et al. (2007)
Cellulose triacetate	100	50 °C	Air sweep	10	2.3	99	Huth et al. (2014)
Cellulose triacetate	30	70 °C	Vacuum	6	2.16	99.9	Prihatiningtyas et al. (2019)
Cellulose acetate	40–140	70 °C	Vacuum	20–25	5.97–3.45	99.7	Naim et al. (2015)
Poly(vinyl alcohol)/polysulfone	30	70.8 °C	Vacuum	0.1–1	7.4	99.9	Chaudhri et al. (2015a)
Poly(vinyl alcohol)/polyacrylonitrile	35	70 °C	Vacuum	2	32.26	99.98	Zhang et al. (2018)
Polyacrylonitrile	35	30 °C	Vacuum	-	24.4	99.9	Austria et al. (2019)
Inorganic							
Silicate-1	3	75 °C	Vacuum	6	11.5	99	Drobek et al. (2012)
Silicate	30–24	80 °C	Air sweep	0.315	4.4–2.4	99.8	Cao et al. (2018)
ZSM-5	3	75 °C	Vacuum	3.3	12.5	99	Drobek et al. (2012)
ZSM-5	38	80 °C	Vacuum	-	0.72	99	Duke et al. (2009)
ZSM-5	30–24	80 °C	Vacuum	0.41	6.28–3.69	99.8	Cao et al. (2018)
Carbon template silica	3	Room temperature	Vacuum	-	3	97	Wijaya et al. (2009)
Carbon template silica	35	Room temperature	Vacuum	0.5	3.7	98.5	Ladewig et al. (2011)
Carbon template silica	40	25 °C	Vacuum	0.21	2.6	99.9	SINGH et al. (2015)
Carbon silica	10–50	60 °C	Vacuum	-	26.5–9.2	99.5–98.6	Yang et al. (2017)
NaA zeolite	Seawater	69 °C	Vacuum	-	1.9	9.9	Cho et al. (2011)
Clinoptilolite	0.1	93 °C	Vacuum	-	2.5	95.8	Swenson et al. (2012)
Clinoptilolite-phosphate	1.4	95 °C	Vacuum	-	15	95	An et al. (2014)
Hydroxyl sodalite	350	200 °C	Vacuum	1	3.9	99.99	Khajavi et al. (2010)
Cobalt oxide silica	10–150	75 °C	Vacuum	0.2–0.35	1.8–0.6	99	Lin et al. (2012)
UiO-66-NH_2	35	44.85–89.85 °C	Air sweep	-	1.5–12.1	99.7	Wan et al. (2017)
La/Y-codoped microporous organosilica	35	25 °C	Vacuum	-	10.3	100	Zhang et al. (2019)

silica NPs concentration in the polymer dope enhances the viscosity (Lalia et al., 2013). which leads to a more thick and more dense membrane with reduced membrane porosity. Xie et al. and Chaudhri et al. found that incorporating SiO_2 in a pervaporation membrane for desalination improved the hydrophilicity of the PV membrane, and thus increased the water flux, while the salt rejection remained above 99% (Xie et al., 2011b; Chaudhri et al., 2018).

2 Graphene oxide (GO)

In recent decades, graphene oxide (GO) has gained a lot of attention in fabrication of nanocomposite membranes for many applications in water treatment, such as desalination, removal of toxic ions and organic molecules (An et al., 2016), and removal of pharmaceutical traces from water and waste water (Carmalin Sophia et al., 2016). Graphene oxide (GO) is a carbon nanomaterial obtained as the oxidized form of graphene. It has hydrophilic properties because it has oxygen containing groups such as carbonyl, hydroxyl, carboxylic and epoxy groups (Zahid et al., 2018). GO has therefore hydrophilic functional groups, such as —NH_2, OH, and S—O_3H (Enotiadis

et al., 2012; Liu et al., 2017), that allow to produce functionalized graphene oxide- and graphene-based materials (Jhaveri and Murthy, 2016). It has been reported that GO shows excellent properties such as high conductivity, large surface area, electromagnetic properties, good tensile and mechanical strength (Zahid et al., 2018), and incorporation of GO in polymeric membranes tends to improve the permeability of such membranes (Xia et al., 2015). Umpong et al. studied the behavior ion and water molecules in the GO nanochannels of the GO membrane during thermally-driven desalination by pervaporation (Cha-Umpong et al., 2020).

Through their simulation results, a new mechanism of ion transport in the GO membrane by the thermal-driven process was found, which can be adjusted by utilizing other cations with higher charge density and high temperature to accelerate the process. Qian et al. investigated the water and salt transport properties, and the desalination performance of the hybrid chitosan/graphene oxide membrane (Qian et al., 2018). They concluded that at a lower GO content, an increment of GO content improved the water transport through the membrane; however, the salt also penetrated the membrane more easily, which resulted in a decrease of the water/salt selectivity. However, an increasing GO loading might lead to the aggregation of GO, which affected the free volume of MMMs and then lead to and increased selectivity. In addition, the optimum water flux was achieved at 1 wt% content of GO due to the increased membrane hydrophilicity and decreased free volume of the membrane. Sun et al. studied the potential of tailoring the microstructure of poly(vinyl alcohol)-intercalated graphene oxide membranes for enhanced desalination performance of high-salinity water by pervaporation.

They concluded that at a lower GO content, an increment of GO content improved the water transport through the membrane; however, the salt also penetrated the membrane more easily, which resulted in a decrease of the water/salt selectivity. However, an increasing GO loading might lead to the aggregation of GO, which affected the free volume of MMMs and then lead to and increased selectivity. In addition, the optimum water flux was achieved at 1 wt% content of GO due to the increased membrane hydrophilicity and decreased free volume of the membrane. Sun et al. studied the potential of tailoring the microstructure of poly(vinyl alcohol)-intercalated graphene oxide membranes for enhanced desalination performance of high-salinity water by pervaporation (Sun et al., 2020). They reported that a high flux of 98.1 kg m^{-2} h^{-1} was obtained for treating a feed solution containing 10 wt% NaCl and 28.3 kg m^{-2} h^{-1} for a saline feed solution with concentration of 20 wt% NaCl (both at 85 °C), while the salt rejection was maintained at 99.99%. Thus, the interlayer spacing and cross-linking network structure between poly(vinyl alcohol) (PVA) and GO were successfully tailored by properly changing PVA intercalation, thus leading to the highest water flux.

However, it has been reported that the water flux depend on the thickness of the GO layer (Nan et al., 2016; Yeh et al., 2013; Chong et al., 2018). Yeh et al. fabricated a multilayered graphene oxide (GO) coated on the thin film nanofibrous composite (TFNC) for ethanol dehydration by pervaporation. The membranes were prepared in the range of 93–600 nm thickness. The results showed that the GO barrier layer thickness of 93 nm obtained a water permeate 200% and the separation factor was nearly four times higher compared to the commercial pervaporation membrane (Yeh et al., 2013). Nan et al. prepared PEI/GO/hPAN nanofiltration membranes for desalination by layer by layer (LbL) assembly of polyethyleneimine (PEI) and GO on the hPAN ultrafiltration membranes as substrate. They found that an increasing GO concentration enhanced the dense layer thickness, which reduces the water flux (Nan et al., 2016).

3 Carbon nanotubes (CNTs)

There has been growing interest in employing CNTs to advance the next generation of membranes. CNTs have been used as nano-additives for water treatment application due to their remarkable chemical inertness and mechanical stability, and high specific surface area with good water transport properties (Das et al., 2014; Kim and Van der Bruggen, 2010). The characteristics of CNTs are that their inside structure tends to act as selective nanopores, hence the CNT-filled membranes exhibit an increased permeability without a decrease in selectivity; moreover, the mechanical and thermal properties are also enhanced (Fontananova et al., 2017). CNTs have been employed for fabricating membranes used in membrane distillation for desalination. CNTs have been integrated with hydrophobic membrane, i.e., polyvinylidene fluoride (PVDF) and polypropylene (PP) and it was reported that these membranes based can be improved to obtain a high membrane performance (Gethard et al., 2011; Roy et al., 2014; Ragunath et al., 2018). Yang et al. investigated poly (vinyl alcohol) (PVA) membranes containing CNTs, produced via interfacial adhesion, hydrogen bonding or covalent bonding to be applied in pervaporation desalination (Yang et al., 2019). The PVA/CNTs membranes were able to enhance the water flux between 38.8%–154.1% compared with the control PVA/MA membrane, while keeping the salt rejection above 99%.

Salt transport behavior was observed by kinetic desorption of NaCl; it was found significantly influenced by the dispersion of CNTs and membrane swelling. Aggregation of CNTs leads to a reduction of the selectivity of the PVA/CNT membrane.

4 Mxene

In 2011, a new family of 2D transition metal carbides, nitrides and carbonitrides called MXenes (pronounced “maxines”) was discovered at Drexel University (Naguib et al., 2014; Hemanth and Kandasubramanian, 2020). MXene is derived from the precursor MAX phase ($M_{n+1}AX_n$), the general formula of MXene is $M_{n+1}X_nT_x$ (n = 1–3), where M is an early transition metal, X is carbon and/or nitrogen, A denotes an element from groups 12 to 16, T is the surface termination groups such as fluorine (–F), oxygen (O), chlorine (Cl), and hydroxyl (O=—H), and x expresses the number of surface functionalities (Ihsanullah, 2020). MXenes and their composites have been applied in many environmental applications including for water purification membranes due to their excellent properties: they have a high hydrophilicity and surface area, and good mechanical and electrical properties (Saththasivam et al., 2019; Zha et al., 2019; Xie et al., 2020). Furthermore, they are promising candidate materials in desalination applications. For example, T_i3C2T_x is hydrophilic with a contact angle of 21.5° and shows an excellent stability in water (Ghidiu et al., 2014). Liu et al. studied ultrathin two-dimensional MXene membranes for pervaporation desalination (Yang et al., 2017).

This was the first time that ultrathin MXene membranes with thickness of ~60 nm were fabricated for pervaporation desalination. The results showed that the membranes had unique 2D interlayer channels as well as a high hydrophilicity. A water flux of 85.4 L m^{-2} h^{-1} was obtained, and salt rejection of 99.5% with a feed concentration of 3.5 wt% NaCl at 65 °C (Liu et al., 2018).

5 Laponite nanoclay (NC-LAP)

Laponite (LAP) is a synthetic nanoclay smectite which the structure and composition closely associated to the natural clay mineral hectorite (Ruzicka and Zaccarelli, 2011; Ding et al., 2016). LAP is consisting of a layered structure with 30 nm diameter and 1 nm in thickness with empirical formula $Na^{+0.7}[(Mg_{5.5}Li_{0.3})\ Si_8\ O_{20}\ (OH)_4]^{-0.7}$. LAP is widely used for various purposes depending on the grade (Selim et al., 2019). Laponite clay is a well-established material for drug delivery, tissue engineering and wound healing applications due to its properties such as high biocompatibility, anisotropic and an excellent surface area (Golafshan et al., 2017; Wang et al., 2012; Perotti et al., 2011). It has been reported that laponite clay exfoliates easily in water, improves the physical properties of hydrogels, and has a high hydrophilicity and a good mechanical strength for nanocomposite polymers (Wassel et al., 2017; Daniel et al., 2008; Morariu et al., 2018; Liu et al., 2014). Selim et al. studied the fabrication of laponite XLG-Poly (vinyl alcohol) (PVA-Lap) mixed matrix membranes (MMMs) for desalination of high-salinity water by pervaporation (Selim et al., 2019). It was found that the MMMs surface hydrophilicity and the mechanical properties enhanced with increasing laponite content. The optimum concentration of laponite was 2%; this showed the highest flux of 58.6 kg m^{-2} h^{-1} and 39.9 kg m^{-2} h^{-1} for a feed solution of 3 wt% NaCl and 10 wt% NaCl, respectively, at 70 °C, with a salt rejection of over 99.9%.

6 Cellulose nanocrystal (CNCs)

Cellulose nanocrystals (CNCs) are a family of cellulosic nanomaterials, which are produced by controlled acidic hydrolysis of cellulose material. CNCs were found in the 1940 s–1950 s, starting when Nickerson and Habrle observed the degradation of cellulosic fibers by hydrolysis process utilized a boiling acidic solutions, and then obtained cellulose sols (Nickerson and Habrle, 1947). Furthermore, by controlling sulfuric acid-catalysis in this hydrolysis process of cellulose fiber, Ranby discovered a colloidal suspensions of cellulosic crystals (Rånby, 1951). CNCs are rod-like acicular nanoparticles with the physical dimensions labelled by length (L), diameter (D), and aspect ratio (L/D). The geometrical dimension depends on the cellulosic source and hydrolysis conditions. CNCs became known as a filler of polymer composite materials in the 2000s (Chakrabarty and Teramoto, 2018). Lately, CNCs have been found attractive to be applied as nanofillers in membrane preparation due to some additional advantages such as natural abundance, low cost, non-toxic, low density, excellent mechanical properties, and easy chemical modification (Dufresne, 2017; Tayeb et al., 2018). However, aggregation of CNCs is a challenge in the fabrication of nanocomposites because they may be incompatible with the polymer, hence some approaches are introduced to obtain the polymer–filler interaction, such as covalent and non-covalent interactions (Chakrabarty and Teramoto, 2018). CNCs have been employed as nanofiller for nanofiltration membranes by Bai et al. They incorporated CNCs into a polyamide (PA) layer for fabricating a novel thin film composite (TFC). The results showed that incorporation of 0.2 wt% CNCs increased the water permeance from 9.52 LMH bar^{-1} to 14.96 LMH bar^{-1} (7.1%), while the selectivity for NaCl increased from 18% to 24% (Bai et al., 2018). Prihatiningtyas et al. prepared CNCs-cellulose triacetate (CTA) nanocomposite membranes for desalination by pervaporation. They found that the optimum concentration of CNCs that can be loaded into a CTA polymer solution was 3 wt%, and the results revealed that the water flux enhanced from 2.16 kg m^{-2} h^{-1} to 5.76 kg m^{-2} h^{-1}] (300%). Furthermore, the water flux was improved by reducing the casting blade height from 200 to 100 μm; a flux of 11.68 kg.m^{-2} h^{-1} was obtained, which was increased by factor of 2, while the NaCl rejection maintained 99.9% (Prihatiningtyas et al., 2019). The incorporation of CNCs in CTA membranes improved the pervaporation performance due to the hydrophilicity of CNCs which have abundant hydroxyl groups, and due to the unique structure of CNCs which changes membrane morphology (Prihatiningtyas et al., 2019).

7 Alumunium dioxide (Al_2O_3)

Aluminum oxide (Al_2O_3) nanoparticles have been used to enhance the hydrophilicity and suppress fouling in polymeric membranes (Dong et al., 2013; Mojtahedi et al., 2013; Ma et al., 2015). Reported studies revealed that as a consequence of hydrophilicity improvement, incorporating Al_2O_3 into a membrane yields a higher water flux than with a neat membrane. In a study on fouling reduction, Arsuaga et al. reported that a high density of Al2O3 NPs on the membrane surface inhibited the deposition/adsorption of Bovine Serum Albumin (BSA) molecules, hence prevented the formation of a fouling layer (María Arsuaga et al., 2013). Al_2O_3 NPs have been used as filler in membranes and applied to remove salt from water. Saleh and Gupta prepared polyamide (PA) nanocomposite membranes containing alumina nanoparticles, then and investigated the performance of these membranes for salt removal by reverse osmosis. The results revealed that the water flux and salt rejection were better than with the neat membrane. The nanocomposite membrane also exhibited a slightly higher rejection of ions compared to the neat membrane (Saleh and Gupta, 2012). Prihatiningtyas et al. employed Al_2O_3 NPs into a CTA membrane to increase the membrane performance for desalination by pervaporation (Prihatiningtyas et al., 2020b). They reported that the hydrophilicity of the nanocomposite membranes improved due to the presence of Al_2O_3 nanoparticles, which finally increased the water flux. However, an increment of the Al_2O_3 content leads to a decrease of the water flux due the aggregation of nanoparticles in the polymer matrix and increasing the membrane thickness, which might hinder the water penetration in the membrane. Incorporating 2% of Al_2O_3 into a CTA membrane was the optimum content: it increased the water flux by 204% compared to pristine membrane, while the salt rejection remained 99.8%. Furthermore, the water flux decreased by 25% without sacrificing the salt rejection, when the concentration of NaCl in the feed solution increased from 30 g/L to 90 g/L.

Nanoparticles (NPs) have attracted growing attention in water treatment; however, toxicity of NPs should be considered for safety as well as the environment.

3.3.2. *Methods of incorporation nanoparticles into polymer matrix*

Literature studies reported that the integration of nanoparticles into polymeric membranes improves the physical and chemical properties, and changes the structure and/or morphology of the membrane (Yin and Deng, 2015; Lakhotia et al., 2018). Generally, there are two methods for incorporation of nanoparticles into a polymer matrix: (1) blending nanoparticles with the casting solution (dope solution) and (2) deposition of nanoparticles on the surface of polymeric membrane (Shahmirzadi and Kargari, 2018).

(a) Blending nanoparticles with dope solution

Nanoparticles (organic or inorganic) and additives are loaded to the dope solution to modify the morphology and performance of the membrane in fabricating the nanocomposite membrane by phase-inversion. The trade-off between thermodynamic enhancement and kinetic hindrance influences the final morphology and performance of the presence of nanoparticles in the membrane (Sadrzadeh and Bhattacharjee, 2013). From a thermodynamic point of view, the addition of nanoparticles into the dope solution reduces the solvent power in the solution and works as a non-solvent agent (Lee et al., 2003), results an instantaneous demixing, then produces a membrane with porous structure (Homayoonfal et al., 2013). Most nanoparticles employed to prepare nanocomposite membrane for desalination are hydrophilic nanoparticles and reduce the miscibility (compatibility) of the polymer/solvent. Hydrophilic nanoparticles increase the diffusional exchange rate between solvent and non-solvent, then accelerate the penetration rate of non-solvent into a polymeric membrane and speed up the demixing process, which results in a porous structure (Homayoonfal et al., 2013). However, an increment of nanoparticles leads to increasing the viscosity of the dope solution, which decreases the diffusional exchange rate between solvent and non-solvent, causing delayed demixing, so that a dense structure is formed (Vatanpour et al., 2011). Incorporating nanoparticles has two opposite effects during the phase inversion process: (1) thermodynamic improvement must be considered since at low-nanoparticles loading, the demixing rate increases, then forms a porous structure. (2) kinetic obstacles must be taken into account due to high-nanoparticles loaded will decrease the diffusional exchange rate between solvent and non-solvent, which results in a dense membrane.

(a) Deposition of nanoparticles on the surface polymer membrane

Depositing nanoparticles on a membrane surface results in surface modified nanocomposite membranes with a thin layer of nanoparticles on a porous support (Namvar-Mahboub and Pakizeh, 2013). A classification of surface modified membranes based on the position of nanoparticles is (i) surface located nanocomposite membranes, (ii) TFC membranes, (iii) TFC with nanocomposite support membranes, and (iv) thin film nanocomposite (TFN) membranes (Shahmirzadi and Kargari, 2018; Lakhotia et al., 2018). Common methods to modify the surface of nanocomposite membrane are (i) self-assembly, (ii) layer-by-layer coating, (iii) chemical grafting, (iv) electrostatic attraction, (v) interfacial polymerization and (vi) UV-assisted-polymerization (Lakhotia et al., 2018). However, the deposition of nanoparticles on the membrane surface has two opposed effects. Although nanoparticles improve the water flux due to the enhancement of hydrophilicity and surface roughness, reducing the pore size decreases the water flux but increases the selectivity (Homayoonfal et al., 2013). Rahimpour et al. compared the deposition of nanoparticles and the blending method (Rahimpour et al., 2008). They concluded that the deposition of nanoparticles is better than blending nanoparticles, because the nanoparticles-deposition method creates stronger physical/chemical bonds, which significantly enhances the membrane performance and anti-fouling ability (Namvar-Mahboub et al., 2014).

3.3.3. *Dispersion of nanoparticles*

The presence of nanoparticles in a polymeric membrane improves the membrane performance for a wide range of membrane processes, from gas separation and pervaporation (Pandey and Chauhan, 2001; Ji and Sikdar, 1996), also nanofiltration and ultrafiltration (Genné et al., 1996; Schaep et al., 1998). However, there are some challenges in incorporation of nanoparticles into polymeric materials; one of them is the dispersion of the nanoparticles in the polymers (Sri Abirami Saraswathi et al., 2019). It has been reported that the dispersion of nanoparticles shows a significant effect on the modifying the membrane morphology. Furthermore, the performance of nanocomposite membranes depends on the size, shape, dispersity, concentration, and interaction between nanoparticles and the membranes (Zahid et al., 2018; Zhao et al., 2015). Dispersion of nanoparticles with diameter less than 100 nm is difficult during membrane fabrication due to the risk of aggregation of nanoparticles caused by weakly surface interactions (Ng et al., 2013). When weakly bound particles are gathering, aggregation or agglomeration occurs, in addition, agglomerates are connected by weak forces, such as van der Waals forces or by simple physical attachment, hence it can be broken down with appropriate external energy (Ng et al., 2013). According to the literature, increasing the concentration of nanoparticles leads to agglomeration of nanoparticles (Prihatiningtyas et al., 2020b; Yu et al., 2009). Gilbert et al. found that ionic strength and pH of the solution enhance the agglomeration of nanoparticles (Gilbert et al., 2009). Agglomeration of nanoparticles is avoided because it yields a poor membrane performance. Studies reported that agglomeration of nanoparticles results in inhomogeneity of the dope solution, which may result in membrane defects. A higher agglomeration causes pore blockage, which leads to a decrease of water permeation (Sotto et al., 2011; Huang et al., 2012). Theoretically, there are two causes of the low dispersity of nanoparticles: (i) incompatibility of nanoparticles with the polymer material and (ii) the agglomeration of nanoparticles in the membrane matrix during phase inversion due to insufficient concentration of additives (Tanahashi and Takeda, 2014). Furthermore, the lack of chemical bonding between the polymer matrices with the nanoadditive also creates a low dispersity and stability of the nanoparticles in the membrane (Thakur and Thakur, 2014). Modification of the nanoparticle surface by chemical treatment and functionalization can improve the dispersion of nanoparticles in the casting dope solutions to obtain the desired performance of nanocomposite membranes (Yao et al., 2017). The functionalization method is based on grafting of functional polymeric molecules to the hydroxyl groups of nanoparticles. Organic acids have been utilized for surface treatment of metal oxide nanoparticles to improve the dispersion in organic solvent as

Table 2 – Hybrid and nanocomposite of PV membranes for desalination.

Membrane	NaCl (g/L)	Operating conditionin feed side	Flux (kg/m^2.h)	Rejection (%)	Ref.
Poly(vinyl alcohol)/maleic acid/silica	2	22 °C	6.93	99.5	Xie et al. (2011b)
Poly(vinyl alcohol)/silica	2	Room temperature	96	99.9	Chaudhri et al. (2015b)
Poly(vinyl alcohol)/silica/polysulfone	2 30	60 °C	20.6 10.6	99.9	Chaudhri et al. (2018)
Poly(vinyl alcohol)-graphene oxide/polyacrylonitrile	35	30 °C 70 °C	18.3 69.1	99.8 99.8	Cheng et al. (2017)
Polyacrylonitrile/ graphene oxide/	35	30 °C 90 °C	14.3 65.1	99.8 99.8	Liang et al. (2015)
Poly(vinyl alcohol)/carbon nantotubes	35	22 °C	6.96	99.91	Yang et al. (2019)
Polyacrylonitrile/MXene	35	65 °C	85.4	99.5	Liu et al. (2018)
Chitosan/graphene oxide	35	81 °C	30	99.99	Qian et al. (2018)
Poly(vinyl alcohol)/glutaraldehyde/Laponite	50	70 °C	58.6	99.9	Selim et al. (2019)
Cellulose triacetate/cellulose nanocrystal	30	70 °C	11.67	99.9	Prihatiningtyas et al. (2020a)
Cellulose triacelate/alumunium oxide	30	70 °C	6.7	99.8	Prihatiningtyas et al. (2020b)
Cellulose triacetate/Ludox-SiO_2	30	70 °C	6.1	99.8	Prihatiningtyas et al. (2020c)

the hydroxyl sites of these nanoparticles are able to react with the carboxylic functional groups in acids (Jalili et al., 2016; Mirabedini et al., 2011). Diminishing the agglomeration problem by grafting different surfactants such as sodium lauryl sulfate (SLS) on the surface of nanoparticles has been reported by Heinz et al. (2017). Iijima et al. revealed that dispersity of nanoparticles in organic solvents could be enhanced by the adsorption of cationic/anionic polymeric dispersants on the nanoparticle surface since the nanoparticles surface will adsorb these dispersants (Morant-Miñana, 2016). Later, steric repulsive forces from the polymer chain are created, which increase the surface charge of the adsorbed nanoparticles, so that nanoparticles will be uniformly distributed in organic solvent medium (Tang et al., 2006). Besides modifying surface nanoparticles, nanoadditive dispersion can be improved by the sol-gel method in the preparation of nanocomposite membranes, which combines the advantages of the traditional immersion precipitation technique and in situ preparation of nanoparticles (Pang et al., 2011). Moreover, the sol–gel method has been reported to enhance the compatibility between nanoparticles with the polymer, allowing to minimize the leaching of nanoparticles from the membranes during filtration (Li et al., 2013b).

3.3.4. *Performance of hybrid and nanocomposite pervaporation membrane for desalination*

At present, much effort is being made to obtain high performance pervaporation membranes by developing new membrane materials. Table 2 summarizes the performance of hybrid and nanocomposite pervaporation membranes for desalination.

4. Conclusion

Desalination by pervaporation has gained much attractiveness due to its performance in terms of water flux, salt rejection, and its reduced thermal requirements. The PV desalination performance depends on the nature and selectivity of the membrane and the nanofiller, diffusivity of the filler, and operating conditions. Current research shows that incorporating nanoparticles in the membrane enhances the performance of PV desalination. Many studies on laboratory and pilot scale have struggled to develop nanocomposite membranes for PV desalination application that can be applied in the industry scale. More studies are needed to develop nanocomposite membrane for PV desalination including producing membranes under practical conditions and with economic feasibility.

Conflict of interest

None declared.

Acknowledgement

This work was supported by the Indonesia Endowment Fund for Education (LPDP). The authors would like to thank to Yusak Hartanto for the fruitful discussions (UCLouvain).

References

Acharya, M., Foley, H.C., 1999. J. Membr. Sci. 161, 1.
Ahmed, F.E., Hashaikeh, R., Hilal, N., 2019. Desalination 453, 54.
Al-Abri, M., Al-Ghafri, B., Bora, T., Dobretsov, S., Dutta, J., Castelletto, S., Rosa, L., Boretti, A., 2019. NPJ Clean Water 2.
Alaei Shahmirzadi, M.A., Kargari, A., 2018. Emerg. Technol. Sustain. Desalin. Handb., 285.
An, W., Zhou, X., Liu, X., Chai, P.W., Kuznicki, T., Kuznicki, S.M., 2014. J. Membr. Sci. 470, 431.
An, D., Yang, L., Wang, T.-J., Liu, B., 2016. Ind. Eng. Chem. Res. 55, 4803.
Austria, H.F.M., Lecaros, R.L.G., Hung, W.-S., Tayo, L.L., Hu, C.-C., Tsai, H.-A., Lee, K.-R., Lai, J.-Y., 2019. Desalination 463, 32.
Bai, L., Liu, Y., Bossa, N., Ding, A., Ren, N., Li, G., Liang, H., Wiesner, M.R., 2018. Environ. Sci. Technol. 52, 11178.
Borisov, I.L., Kujawska, A., Knozowska, K., Volkov, V.V., Kujawski, W., 2018. J. Membr. Sci. 564, 1.
Brüschke, H.E.A., 2006. State-of-the-Art of pervaporation processes in the chemical industry. Membr. Technol., 151–202.
Burshe, M.C., Sawant, S.B., Joshi, J.B., Pangarkar, V.G., 1997. Sep. Purif. Technol. 12, 145.
Cannilla, C., Bonura, G., Frusteri, F., 2017. Catalysts 7.
Cao, Z., Zeng, S., Xu, Z., Arvanitis, A., Yang, S., Gu, X., Dong, J., 2018. Sci. Adv. 4, 1.
Carmalin Sophia, A., Lima, E.C., Allaudeen, N., Rajan, S., 2016. Desalin. Water Treat. 57, 27573.
Chakrabarty, A., Teramoto, Y., 2018. Polymers (Basel) 10.
Chaudhri, S.G., Rajai, B.H., Singh, P.S., 2015a. Desalination 367, 272.
Chaudhri, S.G., Rajai, B.H., Singh, P.S., 2015b. RSC Adv. 5, 65862.
Chaudhri, S.G., Chaudhari, J.C., Singh, P.S., 2018. J. Appl. Polym. Sci. 135, 1.

Cha-Umpong, W., Hosseini, E., Razmjou, A., Zakertabrizi, M., Korayem, A.H., Chen, V., 2020. J. Membr. Sci. 598, 117687.
Cheng, C., Shen, L., Yu, X., Yang, Y., Li, X., Wang, X., 2017. J. Mater. Chem. A: Mater. Energy Sustain. 5, 3558.
Cho, C.H., Oh, K.Y., Kim, S.K., Yeo, J.G., Sharma, P., 2011. J. Membr. Sci. 371, 226.
Chong, J.Y., Wang, B., Mattevi, C., Li, K., 2018. J. Membr. Sci. 549, 385.
Cui, K., Li, P., Zhang, R., Cao, B., 2020. Chem. Eng. Res. Des. 156, 171.
da Silva, D.A.R.O., Zuge, L.C., B.; de Paula Scheer, A., 2020. Sep. Purif. Technol., 116852.
Daniel, L.M., Frost, R.L., Zhu, H.Y., 2008. J. Colloid Interface Sci. 321, 302.
Das, R., Ali, M.E., Hamid, S.B.A., Ramakrishna, S., Chowdhury, Z.Z., 2014. Desalination 336, 97.
Ding, L., Hu, Y., Luo, Y., Zhu, J., Wu, Y., Yu, Z., Cao, X., Peng, C., Shi, X., Guo, R., 2016. Biomater. Sci. 4, 474.
Dong, H., Xiao, K., Li, X., Ren, Y., Guo, S., 2013. Desalin. Water Treat. 51, 3685.
Drioli, E., Stankiewicz, A.I., Macedonio, F., 2011. J. Membr. Sci. 380, 1.
Drobek, M., Yacou, C., Motuzas, J., Julbe, A., Ding, L., Diniz da Costa, J.C., 2012. J. Membr. Sci. 415–416, 816.
Dufresne, A., 2017. Philos. Trans. R. Soc. A: Math. Phys. Eng. Sci. 376, 20170040.
Duke, M.C., O'Brien-Abraham, J., Milne, N., Zhu, B., Lin, J.Y.S., Diniz da Costa, J.C., 2009. Sep. Purif. Technol. 68, 343.
Elimelech, M., Phillip, W.A., 2011. Science (80-) 333, 712.
Enotiadis, A., Angjeli, K., Baldino, N., Nicotera, I., Gournis, D., 2012. Small 8, 3338.
Ercin, A.E., Hoekstra, A.Y., 2014. Environ. Int. 64, 71.
Feng, X., Huang, R.Y.M., 1997. Ind. Eng. Chem. Res. 36, 1048.
Fontananova, E., Grosso, V., Aljlil, S.A., Bahattab, M.A., Vuono, D., Nicoletta, F.P., Curcio, E., Drioli, E., Di Profio, G., 2017. J. Membr. Sci. 541, 198.
Genné, I., Kuypers, S., Leysen, R., 1996. J. Membr. Sci. 113, 343.
Gethard, K., Sae-Khow, O., Mitra, S., 2011. ACS Appl. Mater. Interfaces 3, 110.
Ghidiu, M., Lukatskaya, M.R., Zhao, M.-Q., Gogotsi, Y., Barsoum, M.W., 2014. Nature 516, 78.
Gilbert, B., Ono, R.K., Ching, K.A., Kim, C.S., 2009. J. Colloid Interface Sci. 339, 285.
Golafshan, N., Rezahasani, R., Tarkesh Esfahani, M., Kharaziha, M., Khorasani, S.N., 2017. Carbohydr. Polym. 176, 392.
Hameeteman, E., 2013. Glob. Water Inst., 16.
Han, L.-F., Xu, Z.-L., Cao, Y., Wei, Y.-M., Xu, H.-T., 2011. J. Membr. Sci. 372, 154.
Heinz, H., Pramanik, C., Heinz, O., Ding, Y., Mishra, R.K., Marchon, D., Flatt, R.J., Estrela-Lopis, I., Llop, J., Moya, S., Ziolo, R.F., 2017. Surf. Sci. Rep. 72, 1.
Hemanth, N.R., Kandasubramanian, B., 2020. Chem. Eng. J. 392, 123678.
Homayoonfal, M., Mehrnia, M.R., Mojtahedi, Y.M., Ismail, A.F., 2013. Desalin. Water Treat. 51, 3295.
Hsu, S.T., Cheng, K.T., Chiou, J.S., 2002. Desalination 143, 279.
Huang, J., Arthanareeswaran, G., Zhang, K., 2012. Desalination 285, 100.
Huth, E., Muthu, S., Ruff, L., Brant, J.A., 2014. J. Water Reuse Desalin. 4, 109.
Ihsanullah, I., 2020. Nano-Micro Lett. 12, 1.
Jalili, M.M., Davoudi, K., Zafarmand Sedigh, E., Farrokhpay, S., 2016. Adv. Powder Technol. 27, 2168.
Jhaveri, J.H., Murthy, Z.V.P., 2016. Desalination 379, 137.
Ji, W., Sikdar, S.K., 1996. Ind. Eng. Chem. Res. 35, 1124.
Jiraratananon, R., Chanachai, A., Huang, R.Y.M., Uttapap, D., 2002. J. Membr. Sci. 195, 143.
Khajavi, S., Jansen, J.C., Kapteijn, F., 2010. J. Membr. Sci. 356, 52.
Kim, J., Van der Bruggen, B., 2010. Environ. Pollut. 158, 2335.
Kim, H.-J., Chaikittisilp, W., Jang, K.-S., Didas, S.A., Johnson, J.R., Koros, W.J., Nair, S., Jones, C.W., 2015. Ind. Eng. Chem. Res. 54, 4407.
Kober, P.A., 1917. J. Am. Chem. Soc. 39, 944.
Korin, E., Ladizhensky, I., Korngold, E., 1996. Chem. Eng. Process. Process Intensif. 35, 451.
Korngold, E., Korin, E., 1993. Desalination 91, 187.
Korngold, E., Korin, E., Ladizhensky, I., 1996. Desalination 107, 121.
Kujawa, J., Cerneaux, S., Kujawski, W., 2015. Chem. Eng. J. 260, 43.
Kuznetsov, Y.P., Kruchinina, E.V., Baklagina, Y.G., Khripunov, A.K., Tulupova, O.A., 2007. Russ. J. Appl. Chem. 80, 790.
La, Y.H., Sooriyakumaran, R., Miller, D.C., Fujiwara, M., Terui, Y., Yamanaka, K., McCloskey, B.D., Freeman, B.D., Allen, R.D., 2010. J. Mater. Chem. 20, 4615.
Ladewig, B.P., Tan, Y.H., Lin, C.X.C., Ladewig, K., Diniz da Costa, J.C., Smart, S., 2011. Materials (Basel) 4, 845.
Lakhotia, S.R., Mukhopadhyay, M., Kumari, P., 2018. Sep. Purif. Rev. 47, 288.
Lalia, B.S., Kochkodan, V., Hashaikeh, R., Hilal, N., 2013. Desalination 326, 77.
Lau, W.J., Gray, S., Matsuura, T., Emadzadeh, D., Paul Chen, J., Ismail, A.F., 2015. Water Res. 80, 306.
Lee, K.-W., Seo, B.-K., Nam, S.-T., Han, M.-J., 2003. Desalination 159, 289.
Lee, K.P., Arnot, T.C., Mattia, D., 2011. J. Membr. Sci. 370, 1.
Li, P., 2016. Polym. Sci. 2, 100014.
Li, P., Chen, H.Z., Chung, T.-S., 2013a. J. Membr. Sci. 434, 18.
Li, Y., He, G., Wang, S., Yu, S., Pan, F., Wu, H., Jiang, Z., 2013b. J. Mater. Chem. A Mater. Energy Sustain 1, 10058.
Li, L., Hou, J., Ye, Y., Mansouri, J., Chen, V., 2017. Desalination 422, 49.
Li, Q., Cao, B., Li, P., 2018. Ind. Eng. Chem. Res. 57, 11178.
Li, X., Molelekwa, G.F., Khellouf, M., Van der Bruggen, B., Gonçalves, G.A.B., Marques, P. (Eds.), 2019. Nanostructured Materials for Treating Aquatic Pollution. Springer International Publishing, Cham, p. 243.
Liang, B., Pan, K., Li, L., Giannelis, E.P., Cao, B., 2014. Desalination 347, 199.
Liang, B., Zhan, W., Qi, G., Lin, S., Nan, Q., Liu, Y., Cao, B., Pan, K., 2015. J. Mater. Chem. A 3, 5140.
Liang, B., Li, Q., Cao, B., Li, P., 2018. Desalination 433, 132.
Lin, C.X.C., Ding, L.P., Smart, S., Diniz da Costa, J.C., 2012. J. Colloid Interface Sci. 368, 70.
Liu, S.X., Vane, L.M., Peng, M., 2003. J. Hazard. Subst. Res. 4, 1.
Liu, W., Yee, S., Adanur, S., 2014. J. Text. Inst. 105, 423.
Liu, G., Han, K., Ye, H., Zhu, C., Gao, Y., Liu, Y., Zhou, Y., 2017. Chem. Eng. J. 320, 74.
Liu, G., Shen, J., Liu, Q., Liu, G., Xiong, J., Yang, J., Jin, W., 2018. J. Membr. Sci. 548, 548.
Luis, P., 2018. Pervaporation. Elsevier Inc.
Ma, B., Hu, C., Wang, X., Xie, Y., Jefferson, W.A., Liu, H., Qu, J., 2015. J. Membr. Sci. 492, 88.
Malekpour, A., Millani, M.R., Kheirkhah, M., 2008. Desalination 225, 199.
María Arsuaga, J., Sotto, A., del Rosario, G., Martínez, A., Molina, S., Teli, S.B., de Abajo, J., 2013. J. Membr. Sci. 428, 131.
Maus, E., Brüschke, H.E.A., 2002. Desalination 148, 315.
McGinnis, R.L., Elimelech, M., 2007. Desalination 207, 370.
Meng, J., Li, P., Cao, B., 2019. ACS Appl. Mater. Interfaces 11, 28461.
Meng, J., Lau, C.H., Xue, Y., Zhang, R., Cao, B., Li, P., 2020. J. Mater. Chem. A 8, 8462.
Mirabedini, S.M., Sabzi, M., Zohuriaan-Mehr, J., Atai, M., Behzadnasab, M., 2011. Appl. Surf. Sci. 257, 4196.
Mojtahedi, Y.M., Mehrnia, M.R., Homayoonfal, M., 2013. Desalin. Water Treat. 51, 6736.
Morant-Miñana, M.C., 2016. Encycl. Biomed. Polym. Polym. Biomater. 27, 5569.
Morariu, S., Bercea, M., Brunchi, C.-E., 2018. J. Appl. Polym. Sci. 135, 46661.
Naguib, M., Mochalin, V.N., Barsoum, M.W., Gogotsi, Y., 2014. Adv. Mater. 26, 992.
Naim, M., Elewa, M., El-Shafei, A., Moneer, A., 2015. Water Sci. Technol. 72, 785.
Namvar-Mahboub, M., Pakizeh, M., 2013. Sep. Purif. Technol. 119, 35.
Namvar-Mahboub, M., Pakizeh, M., Davari, S., 2014. J. Membr. Sci. 459, 22.

Nan, Q., Li, P., Cao, B., 2016. Appl. Surf. Sci. 387, 521.
Ng, L.Y., Mohammad, A.W., Leo, C.P., Hilal, N., 2013. Desalination 308, 15.
Nickerson, R.F., Habrle, J.A., 1947. Ind. Eng. Chem. 39, 1507.
Ong, Y.K., Shi, G.M., Le, N.L., Tang, Y.P., Zuo, J., Nunes, S.P., Chung, T.S., 2016. Prog. Polym. Sci. 57, 1.
Oren, Y., 2008. Desalination 228, 10.
Pandey, P., Chauhan, R.S., 2001. Prog. Polym. Sci. 26, 853.
Pang, R., Li, J., Wei, K., Sun, X., Shen, J., Han, W., Wang, L., 2011. J. Colloid Interface Sci. 364, 373.
Peng, F., Lu, L., Sun, H., Jiang, Z., 2006. J. Membr. Sci. 281, 600.
Perotti, G.F., Barud, H.S., Messaddeq, Y., Ribeiro, S.J.L., Constantino, V.R.L., 2011. Polymer (Guildf) 52, 157.
Prihatiningtyas, I., Volodin, A., Van der Bruggen, B., 2019. Ind. Eng. Chem. Res. 58, 14340.
Prihatiningtyas, I., Li, Y., Hartanto, Y., Vananroye, A., Coenen, N., Van der Bruggen, B., 2020a. Chem. Eng. J. 388.
Prihatiningtyas, I., Gebreslase, G.A., Van der Bruggen, B., 2020b. Desalination 474, 114198.
Prihatiningtyas, I., Hartanto, Y., Ballesteros, M.S.R., Van der Bruggen, B., 2020c. J. Appl. Polym. Sci., http://dx.doi.org/10.1002/app.50000, In press.
Purkait, M.K., Sinha, M.K., Mondal, P., Singh, R., 2018. Introduction to Membranes, vol. 25.
Qian, X., Li, N., Wang, Q., Ji, S., 2018. Desalination 438, 83.
Quiñones-Bolaños, E., Zhou, H., Soundararajan, R., Otten, L., 2005. J. Membr. Sci. 252, 19.
Ragunath, S., Roy, S., Mitra, S., 2018. Sep. Purif. Technol. 194, 249.
Rahimpour, A., Madaeni, S.S., Taheri, A.H., Mansourpanah, Y., 2008. J. Membr. Sci. 313, 158.
Rahman, I.A., Padavettan, V., 2012. J. Nanomater. 2012, 132424.
Rallini, M., Kenny, J.M., 2017. Nanofillers in Polymers. Elsevier Inc.
Rånby, B.G., 1951. Discuss. Faraday Soc. 11, 158.
Roy, S., Singha, N.R., 2017. Membranes (Basel) 7.
Roy, S., Bhadra, M., Mitra, S., 2014. Sep. Purif. Technol. 136, 58.
Ruzicka, B., Zaccarelli, E., 2011. Soft Matter 7, 1268.
Sadrzadeh, M., Bhattacharjee, S., 2013. J. Membr. Sci. 441, 31.
Sadrzadeh, M., Mohammadi, T., 2008. Desalination 221, 440.
Saeed, M., Rafiq, S., Bergersen, L.H., Deng, L., 2017. Sep. Purif. Technol. 179, 550.
Saleh, T.A., Gupta, V.K., 2012. Sep. Purif. Technol. 89, 245.
Sani, N.A.A., Lau, W.J., Ismail, A.F., 2015. Korean J. Chem. Eng. 32, 743.
Saththasivam, J., Wang, K., Yiming, W., Liu, Z., Mahmoud, K.A., 2019. RSC Adv. 9, 16296.
Schaep, J., Vandecasteele, C., Leysen, R., Doyen, W., 1998. Sep. Purif. Technol. 14, 127.
Selim, A., Toth, A.J., Haaz, E., Fozer, D., Szanyi, A., Hegyesi, N., Mizsey, P., 2019. Sep. Purif. Technol. 221, 201.
Semiat, R., 2008. Environ. Sci. Technol. 42, 8193.
Shahmirzadi, M.A.A., Kargari, A., 2018. Nanocomposite Membranes. Elsevier Inc.
Shao, P., Huang, R.Y.M., 2007. J. Membr. Sci. 287, 162.
Shieh, J.-J., Chung, T.-S., Paul, D.R., 1999. Chem. Eng. Sci. 54, 675.
SINGH, P.S., CHAUDHRI, S.G., KANSARA, A.M., SCHWIEGER, W., SELVAM, T., REUSS, S., ASWAL, V.K., 2015. Bull. Mater. Sci. 38, 565.
Slater, C.S., Schurmann, T., MacMillian, J., Zimarowski, A., 2006. Sep. Sci. Technol. 41, 2733.
Sotto, A., Boromand, A., Balta, S., Kim, J., Van Der Bruggen, B., 2011. J. Mater. Chem. 21, 10311.
Sri Abirami Saraswathi, M.S., Nagendran, A., Rana, D., 2019. J. Mater. Chem. A 7, 8723.
Sule, M., Jiang, J., Templeton, M., Huth, E., Brant, J., Bond, T., 2013. Environ. Technol. 34, 1329.
Sun, J., Qian, X., Wang, Z., Zeng, F., Bai, H., Li, N., 2020. J. Membr. Sci. 599.
Swenson, P., Tanchuk, B., Gupta, A., An, W., Kuznicki, S.M., 2012. Desalination 285, 68.
Taha, A.A., Wu, Y., Wang, H., Li, F., 2012. J. Environ. Manage. 112, 10.
Tanahashi, M., Takeda, K., 2014. J. Nanosci. Nanotechnol. 14, 3123.
Tang, F., Uchikoshi, T., Ozawa, K., Sakka, Y., 2006. J. Eur. Ceram. Soc. 26, 1555.
Tayeb, A.H., Amini, E., Ghasemi, S., Tajvidi, M., 2018. Molecules 23, 1.
Thakur, V.K., Thakur, M.K., 2014. Carbohydr. Polym. 109, 102.
Tusel, G.F., Brüschke, H.E.A., 1985. Desalination 53, 327.
Vatanpour, V., Madaeni, S.S., Moradian, R., Zinadini, S., Astinchap, B., 2011. J. Membr. Sci. 375, 284.
Vatanpour, V., Madaeni, S.S., Khataee, A.R., Salehi, E., Zinadini, S., Monfared, H.A., 2012. Desalination 292, 19.
Vörösmarty, C.J., Green, P., Salisbury, J., Lammers, R.B., 2000. Science (80-) 289, 284.
Wan, L., Zhou, C., Xu, K., Feng, B., Huang, A., 2017. Micropor. Mesopor. Mater. 252, 207.
Wang, S., Zheng, F., Huang, Y., Fang, Y., Shen, M., Zhu, M., Shi, X., 2012. ACS Appl. Mater. Interfaces 4, 6393.
Wang, Q., Li, N., Bolto, B., Hoang, M., Xie, Z., 2016. Desalination 387, 46.
Wang, Z., Ma, H., Chu, B., Hsiao, B.S., 2017. J. Appl. Polym. Sci. 134, 1.
Wassel, E., Es-Souni, M., Berger, N., Schopf, D., Dietze, M., Solterbeck, C.-H., Es-Souni, M., 2017. Langmuir 33, 6739.
Wijaya, S., Duke, M.C., Diniz da Costa, J.C., 2009. Desalination 236, 291.
Wijmans, J.G., Athayde, A.L., Daniels, R., Ly, J.H., Kamaruddin, H.D., Pinnau, I., 1996. J. Membr. Sci. 109, 135.
Wittbecker, E.L., Morgan, P.W., 1959. J. Polym. Sci. 40, 289.
Wu, H., Mansouri, J., Chen, V., 2012. Procedia Eng. 44, 355.
Wu, D., Gao, A., Zhao, H., Feng, X., 2018. Chem. Eng. Res. Des. 136, 154.
Xia, S., Yao, L., Zhao, Y., Li, N., Zheng, Y., 2015. Chem. Eng. J. 280, 720.
Xie, Z., Ng, D., Hoang, M., Duong, T., Gray, S., 2011a. Desalination 273, 220.
Xie, Z., Hoang, M., Duong, T., Ng, D., Dao, B., Gray, S., 2011b. J. Membr. Sci. 383, 96.
Xie, Z., Hoang, M., Ng, D., Doherty, C., Hill, A., Gray, S., 2014. Sep. Purif. Technol. 127, 10.
Xie, Z., Li, N., Wang, Q., Bolto, B., 2018. Emerg. Technol. Sustain. Desalin. Handb., 205.
Xie, Z., Peng, Y.-P., Yu, L., Xing, C., Qiu, M., Hu, J., Zhang, H., 2020. Sol. RRL 4, 1900400.
Xu, G.R., Wang, J.N., Li, C.J., 2013. Desalination 328, 83.
Xue, Ylong, Lau, C.H., Cao, B., Li, P., 2019. J. Membr. Sci. 575, 135.
Xue, Y.L., Huang, J., Lau, C.H., Cao, B., Li, P., 2020. Nat. Commun. 11.
Yang, H., Elma, M., Wang, D.K., Motuzas, J., Diniz da Costa, J.C., 2017. J. Membr. Sci. 523, 197.
Yang, G., Xie, Z., Cran, M., Ng, D., Gray, S., 2019. J. Membr. Sci. 579, 40.
Yao, H., Hawkins, S.A., Sue, H.-J., 2017. Compos. Sci. Technol. 146, 161.
Yave, W., Car, A., Funari, S.S., Nunes, S.P., Peinemann, K.-V., 2010. Macromolecules 43, 326.
Yeh, T.M., Wang, Z., Mahajan, D., Hsiao, B.S., Chu, B., 2013. J. Mater. Chem. A 1, 12998.
Yeom, C.K., Lee, K.-H., 1997. J. Membr. Sci. 135, 225.
Yin, J., Deng, B., 2015. J. Membr. Sci. 479, 256.
Yu, L.-Y., Xu, Z.-L., Shen, H.-M., Yang, H., 2009. J. Membr. Sci. 337, 257.
Zahid, M., Rashid, A., Akram, S., Rehan, Z.A., Razzaq, W., 2018. J. Membr. Sci. Technol. 08, 1.
Zha, X.-J., Zhao, X., Pu, J.-H., Tang, L.-S., Ke, K., Bao, R.-Y., Bai, L., Liu, Z.-Y., Yang, M.-B., Yang, W., 2019. ACS Appl. Mater. Interfaces 11, 36589.
Zhang, R., Xu, X., Cao, B., Li, P., 2018. Pet. Sci. 15, 146.
Zhang, H.Y., Wen, J.L., Shao, Q., Yuan, A., Ren, H.T., Luo, F.Y., Zhang, X.L., 2019. J. Membr. Sci. 584, 353.
Zhao, S., Yan, W., Shi, M., Wang, Z., Wang, J., Wang, S., 2015. J. Membr. Sci. 478, 105.
Zhao, P., Xue, Y., Zhang, R., Cao, B., Li, P., 2020. J. Membr. Sci. 611, 118367.
Zwijnenberg, H.J., Koops, G.H., Wessling, M., 2005. J. Membr. Sci. 250, 235.

Nanocomposite pervaporation membrane for desalination

ORIGINALITY REPORT

11%	6%	12%	2%
SIMILARITY INDEX	INTERNET SOURCES	PUBLICATIONS	STUDENT PAPERS

MATCH ALL SOURCES (ONLY SELECTED SOURCE PRINTED)

6%

★ Qinzhuo Wang, Na Li, Brian Bolto, Manh Hoang, Zongli Xie. "Desalination by pervaporation: A review", Desalination, 2016

Publication

Exclude quotes	On	Exclude matches	< 2%
Exclude bibliography	On		